Targeting mechanoresponsive proteins in pancreatic cancer: 4-hydroxyacetophenone blocks dissemination and invasion by activating MYH14

Alexandra Surcel[1],[*], Eric S. Schiffhauer[1], Dustin G. Thomas[1], Qingfeng Zhu[2], Kathleen T. DiNapoli[1],[3], Maik Herbig[4], Oliver Otto[4],[†], Hoku West-Foyle[1], Angela Jacobi[4], Martin Kräter[4], Katarzyna Plak[4], Jochen Guck[4], Elizabeth M. Jaffee[5], Pablo A. Iglesias[1],[3], Robert A. Anders[2], Douglas N. Robinson[1],[6],[7],[*]

[1]Department of Cell Biology, Johns Hopkins University School of Medicine, Baltimore, MD 21205, USA

[2]Department of Pathology, Johns Hopkins University School of Medicine, Baltimore, MD 21205, USA

[3]Department of Electrical and Computer Engineering, Johns Hopkins University Whiting School of Engineering, Baltimore, MD 21218, USA

[4]Biotechnology Center, Center for Molecular and Cellular Bioengineering, Technische Universität Dresden, 01307 Dresden, Germany

[5]Department of Oncology, Sidney Kimmel Cancer Center at Johns Hopkins, The Skip Viragh Pancreatic Cancer Center, and the Bloomberg Kimmel Institute, Johns Hopkins University, Baltimore, MD 21205, USA

[6]Department of Pharmacology and Molecular Sciences, Johns Hopkins University School of Medicine, Baltimore, MD 21205, USA

[7]Department of Medicine, Johns Hopkins University School of Medicine, Baltimore, MD 21205, USA

Abstract

Metastasis is complex, involving multiple genetic, epigenetic, biochemical, and physical changes in the cancer cell and its microenvironment. Cells with metastatic potential are often characterized by altered cellular contractility and deformability, lending them the flexibility to disseminate and navigate through different microenvironments. We demonstrate that mechanoresponsiveness is a hallmark of pancreatic cancer cells. Key mechanoresponsive proteins, those that accumulate in

[*]**To whom correspondence should be addressed:** Alexandra Surcel, Department of Cell Biology, 725 N. Wolfe St., Baltimore, MD 21205, asurcel1@jhmi.edu, Douglas N. Robinson, Department of Cell Biology, 725 N. Wolfe St., Baltimore, MD 21205, dnr@jhmi.edu.
[†]Current address: Centre for Innovation Competence, Humoral Immune Reactions in Cardiovascular Diseases Biomechanics, University of Greifswald, 17489 Greifswald, Germany

response to mechanical stress, specifically nonmuscle myosin IIA (MYH9) and IIC (MYH14), α-actinin 4, and filamin B, were highly expressed in pancreatic cancer as compared to healthy ductal epithelia. Their less responsive sister paralogs - myosin IIB (MYH10), α-actinin 1, and filamin A - had lower expression or disappeared with cancer progression. We demonstrate that proteins whose cellular contributions are often overlooked due to their low abundance, can have profound impact on cell architecture, behavior, and mechanics. Here, the low abundant protein MYH14 promoted metastatic behavior and could be exploited with 4-hydroxyacetophenone (4-HAP), which increased MYH14 assembly, stiffening cells. As a result, 4-HAP decreased dissemination, induced cortical actin belts in spheroids, and slowed retrograde actin flow. 4-HAP also reduced liver metastases in human pancreatic cancer-bearing nude mice. Thus, increasing MYH14 assembly overwhelms the ability of cells to polarize and invade, suggesting targeting the mechanoresponsive proteins of the actin cytoskeleton as a new strategy to improve the survival of pancreatic cancer patients.

Introduction

Altered mechanical states of cells and tissues underlie morphological changes concomitant with cancer progression (1–6). Cells undergo shifts in their contractility and deformability, with the latter positively or negatively correlated with aggressiveness and patient outcome, depending on cancer type. Physical changes in the extracellular matrix (ECM) of the stroma and alterations in the cellular composition of tumor microenvironments are established promoters of aggressive cancer behavior (7–10). In addition, as cancer cells move from the primary tissue environment to distal locations through dissemination, invasion, and finally the establishment of metastatic niches, they experience a broad range of external environments. Thus, metastasis occurs at the interface of how a cell physically interacts with a changing mechanical landscape – these interactions are likely dependent on a cell's intrinsic adaptability to sense and respond to these mechanical changes (11). We anticipate that this cellular adaptability allows the cell to tune its mechanical state and force-generating capability as needed and depends on the cell's highly dynamic toolbox of mechanoresponsive proteins (defined here as those having the ability to redistribute in response to mechanical stress (12,13)). This toolbox, along with its regulatory components, collectively constitutes the mechanobiome.

The mechanobiome is the network of proteins that defines the cell's mechanical properties, generates forces, integrates chemical and mechanical cues, and feeds this information back onto other cellular processes, such as gene expression and metabolism (14–17). These proteins affect cell mechanics through active force generation that results from actin assembly that pushes outward on the membrane and myosin II-mediated contractility that pulls inward on the membrane (18). Myosin II-mediated contractility also depends on other actin crosslinking proteins in the cytoskeletal network, and their cross-talk fine-tunes the deformability and contractility of the cell (12). Unsurprisingly, this mechanical network undergoes striking changes in expression during cancer progression, which facilitates the dramatic spatial and temporal reorganization of the cytoskeleton in a metastatic cell. Varying protein levels of critical components of the mechanobiome and the broader actin cytoskeleton have been observed in a wide range of cancers (19–30). In addition, major

cancer drivers and signaling proteins have altered expression patterns and additionally impact cell mechanics. Yes-Associated Protein (YAP), whose overexpression is associated with numerous cancers (31), modulates cellular actin architecture and nonmuscle myosin II regulatory light chain expression and phosphorylation, in turn affecting mechanical parameters, specifically cortical tension and deformability (32). Early activating KRAS mutations that occur in over 90% of pancreatic cancers, and at high rates in colorectal and lung cancers, lead to increased deformability and altered contractility (33,34). Overexpression of members of the 14-3-3 family is negatively correlated with prognosis for glioblastoma (35) and liver (36), pancreatic (37), and lung (38) cancer patients. While 14-3-3 proteins are involved in numerous biological processes, they also modulate nonmuscle myosin II bipolar filament assembly and cell mechanics (39,40). Furthermore, a key inhibitor of myosin II, the myosin light chain phosphatase subunit MYPT1, is highly upregulated in pancreatic cancer (41).

Here we use a battery of model systems, from *Dictyostelium* to human patient samples, to test the concept that the upregulation of mechanoresponsive proteins may be harnessed for small molecule manipulation with the goal of returning an invasive cell to a more stable, non-invasive state (Fig. S1). To accomplish this, we first demonstrate that mechanoresponsive proteins are upregulated in patient-derived pancreatic cancer tissue samples and cell lines, and that these proteins directly impact cell mechanics. We find that altered pancreatic ductal adenocarcinoma cancer (PDAC) mechanics emanate in part from a changing ratio of nonmuscle myosin IIs, wherein myosin IIA (MYH9) and IIC (MYH14) are upregulated while myosin IIB (MYH10) is downregulated. We quantify the concentration of nonmuscle myosin paralogs in pancreatic cancer cells, and find that despite its relatively low concentration, myosin IIC has a significant impact on single cell behavior and collective behavior in tissue spheroids. We then demonstrate that an upregulated mechanoresponsive protein can be used as a pharmacological target, by using a small molecule mechanical modulator, 4-hydroxyacetophenone (4-HAP), which we previously discovered increases the assembly of myosin IIC and stiffens PDAC cells (42). Since then, others have shown that 4-HAP increases the stiffness of breast cancer cells (43). We find that 4-HAP induces cortical actin belts and increases transverse actin arcs in single cells and tissue spheroids in a myosin IIC-dependent manner. This 4-HAP-induced change in cytoskeletal structure and mechanics leads to a decrease in PDAC metastasis in a mouse liver metastasis model. In Bryan *et al.* (submitted for publication), 4-HAP also reduces metastasis in a colorectal cancer model. Thus, we collectively demonstrate that specifically targeting mechanoresponsive proteins by increasing their activity (in this case by promoting myosin IIC assembly), has therapeutic potential for patients.

Materials and Methods

Statistical Analysis

Parametric and nonparametric analyses were used throughout the study. For continuous distribution data sets, we used either the Student t test or the Mann Whitney Wilcoxon test for two groups. For multiple groups, either ANOVA followed by Fisher's Least Square Difference post hoc test or the Kruskal Wallis followed by the Mann Whitney Wilcoxon was

used. For two groups characterized as a frequency (percentage), we used Comparison of Proportions. We used KaleidaGraph (Synergy Software), R, or manual calculation. The tests used are described in individual methods sections and in figure legends. P values are presented either in the figure legend or figure panels.

Cell culture and strains

Parental pancreatic cell lines—Human pancreatic ductal epithelial cells (HPDE) were obtained from Dr. Ming-Sound Tsao (University of Toronto, Ontario Canada), and human primary tumor-derived cells (Panc10.05), human metastatically-derived cells (AsPC-1), and human-derived HeLa cells were purchased from ATCC. The Panc4.03 cell line was established in the Jaffee lab. All were grown using standard cell culture methods. HPDE cells were grown in Keratinocyte media (Gibco) with 1% penicillin and streptomycin, while Panc10.05, Panc02, Panc4.03, and AsPC-1 cells were grown in RPMI 1640, L-Glutamine media (Gibco) supplemented with 1% penicillin and streptomycin, sodium pyruvate (Gibco), non-essential amino acids (Gibco), 10% FBS (ATLAS Bio), and 0.2% insulin. HeLa cells were grown in DMEM (Gibco) with 1% penicillin and streptomycin and 10% FBS (ATLAS Bio). In accordance with NIH guidelines, cell lines were authenticated using short tandem repeat profiling at the genetic recourses core facility at Johns Hopkins University. Routine *Mycoplasma* testing was performed by MycoAlert *Mycoplasma* Detection Kit (catalog no. LT07–118) every 3–6 months. Cell lines were grown for no more than 10 passages in all experiments.

Immunohistochemistry of patient samples—The human tissue was collected and evaluated under JHH IRB #NA_00001584. Human pancreatic cancer samples were fixed in formalin, paraffin embedded, and processed for routine histology. Additional 5-μm sections were cut onto plus slides and baked prior to IHC staining. Details of the antibodies and methods for staining are provided in the Supplemental Materials and Methods. Quantitative analysis of tissue samples (Fig. S2A) across stages of cancer progression (Fig. S2B), plus expression pattern data from the Gene Expression Omnibus (Fig. S2C) are shown in the Supplement.

Engineered cell lines—Both lentiviral knockdown and adenoviral overexpression cell lines were generated in Panc10.05, and in some cases AsPC-1 and HDPE parental strains. For lentiviral knockdown, the hairpins used (Sigma Mission shRNA) were selected after having analyzed a minimum of three shRNAs for each gene:

shCTRL NT control: 5′-CAACAAGATGAAGAGCACCAA-3′

shIIA: 5'-GCCAAGCTCAAGAACAAGCAT-3'

shIIC: 5'-GCTCAAATATGAGGCCACAAT-3'

shACTN4: 5'-CAGGACATGTTCATCGTCCAT-3'

shFLNB: 5'-GCTGACATTGAAATGCCCTTT-3'

Target plasmids were co-transfected with generation 2.0 lentiviral packaging plasmids psPAX.2 and pMD2.G via Transit 20/20 (Mirrus) transfection reagent into Lenti-X

HEK293t cells. Sixteen hours after transfection, the media was changed to fresh DMEM (10% FBS/1% penicillin-streptomycin). Virus-containing media was harvested after an additional 24 hrs for lentiviral infection to target cells. Positively infected cells were then selected for with 1 or 5 ng/ml puromycin in Panc10.05 or AsPC-1 cells respectively, for 5 days as determined by kill-curve analysis. Quantification of expression in control and knockdown lines was confirmed by western analysis and CqPCR (Fig. S3).

For overexpression using the adenoviral system, fluorescent adenovirus for the expression of GFP-MYH9, GFP-MYH10, MYH14-GFP, mCherry-ACTN1, GFP-ACTN4, and GFP control were purchased from Vector BioLabs, Malvern, PA. Optimal multiplicity of infection (MOI= # of virus particles/cell) was first calculated by plating equal numbers of cells in a 96-well plate, then titrating virus between 0 and 200 MOI and observing fluorescence and cell death at 48 hours. For the myosins, the optimal MOI was found to be 50, where cell death was not seen and the percent of fluorescent cells was highest. While an MOI of 50 showed the highest expression and no death for the α-actinin constructs, the amount of protein expressed in cells was extremely high by western analysis, and so the MOI was lowered to 10. For all studies, an MOI of 50 was used for the GFP control. The filamin A and filamin B genes were too large to insert in an adenoviral vector with a fluorescent reporter. For mechanoresponse experiments on filamin A and filamin B or myosinIIC$_{pep}$, AsPC-1 and HeLa cells respectively were transiently transfected with FuGene HD transfection reagent (Promega, Madison, WI) using 1 μg of DNA for each plasmid and imaged 36 hrs post-transfection. The filamin A plasmid, pmdsRed-FLNA, was a gift from Fumihiko Nakamura. The filamin B plasmid, EGFP-FLNB-pCI-C1, was a gift from Arnoud Sonnenberg. The myosinIIC$_{pep}$ was constructed as described in the Supplemental Materials and Methods.

Experimental setup and analysis

The cell lines described above were used throughout the study across multiple experimental designs. Detailed methods for immunohistochemistry with patient-derived samples (including antibodies, reagents, preparation, staining, scoring and analysis), quantification of cellular myosin II paralog concentrations, mechanoresponse and mechanics measurements via MPA and RT-DC, 2D random migration, actin retrograde flow, transwell assays, tissue spheroids (generation, staining, and quantification), and mouse hemisplenectomies (IACUC protocol #M014M94) can be found in the Supplemental Materials and Methods.

Results

Mechanoresponsive machinery is upregulated in pancreatic cancer

Using the social amoeba *Dictyostelium discoideum*, we previously identified ten mechanoresponsive proteins from a survey of ~35 proteins that accumulate in varying degrees to externally applied mechanical pressure (12,44,45). With these ten, we used mathematical modeling to develop a physical theory to explain the accumulation of three critical structural elements across phyla – nonmuscle myosin II, α-actinin, and filamin (12,46). Our theory also predicted which paralogs of these proteins found in mammals were mechanoresponsive (13). To determine if these mechanoresponsive proteins have similar

function in human disease, we assessed their localization in human pancreatic cancer cell lines in response to applied external stress by using micropipette aspiration (MPA) (Fig. 1). Fluorescently labeled myosin IIA (MYH9), IIB (MYH10), and IIC (MYH14), as well as the actin crosslinkers α-actinin 1 (ACTN1), α-actinin 4 (ACTN4), filamin A (FLNA), and filamin B (FLNB) were transiently expressed in several cell lines. These cell lines included HPDE (immortalized Human Pancreatic Ductal Epithelial cells), Panc10.05 (stage II pancreatic adenocarcinoma-derived), and AsPC-1 (stage IV ascites-metastasis-derived) (Fig. 1A). Cells were deformed for five minutes at a pressure of 0.3 nN/μm^2, and the maximal protein accumulation in response to the dilational deformation at the aspirated tip of the cell was quantified by normalizing the fluorescence intensity at the tip region (I_p) to the unstressed cortex opposite of the pipette (I_o) (Fig. 1B).

Myosin IIA and myosin IIC were mechanoresponsive in all cell lines relative to GFP-only controls, whereas myosin IIB showed no accumulation, consistent with its previously observed cell-type-specific mechanoresponsiveness (Fig. 1A, B) (13,47). Because myosin IIA, IIB, and IIC can co-assemble in cells (48), we then tested how the paralogs might influence each other's mechanoresponsiveness and found that each paralog's mechanoresponsiveness was independent of the other paralogs (Fig. 1C, D).

Of the α-actinins, α-actinin 4, but not α-actinin 1, was mechanoresponsive, especially in Panc10.05 and AsPC-1 cells. This differential behavior between the α-actinin paralogs likely results from the much lower actin binding affinity of the actin binding domain of α-actinin 4 (K_d=32 μM) compared to that of α-actinin 1 (K_d=0.36 μM). This affinity differential leads to a more dynamic α-actinin 4 behavior that is necessary for the protein to respond to mechanical stress (13). As we predicted, the scenario for filamins differs with regard to actin binding affinity because cooperativity now plays a role (12,13). In this case, filamin B (K_d=7 μM) showed a stronger mechanoresponse than filamin A (K_d=17 μM) did (Fig. 1) (13).

We hypothesized that the mechanoresponsive machinery is upregulated concomitant with cancer initiation and progression to endow cells with the ability to sense and respond to changing physical environments across discrete tissue types. To test this idea, we performed immunohistochemistry on pancreatic cancer tissue samples from 20 patients across all seven proteins – the three nonmuscle myosin IIs (IIA, IIB, and IIC), the two α-actinins (1 and 4), and the two filamins (A and B). We compared normal ducts with cancerous ducts in primary and metastatic lesions. In addition, we derived a scoring system that allowed us to delineate between high expression and low expression, as well as percentage of cells positively stained within the quantified ducts (outlined in Fig. S2A). All mechanoresponsive proteins showed a significant increase in expression in cancerous versus normal ducts (Fig. 2A, Fig. S2B), quantified in Fig. 2B. Myosin IIA and myosin IIC increased in expression, with myosin IIC specifically upregulated in the adenocarcinoma, while myosin IIA increased across the pancreatic cancer stroma in addition to the ducts. The non-mechanoresponsive myosin IIB showed no significant change in expression, with very little staining in both normal and cancerous pancreatic tissues. The mechanoresponsive α-actinin 4 also increased in expression in the ducts, concurrent with cancer progression, while α-actinin 1 maintained mostly uniform expression levels across all ducts. Filamin B, which is also highly

mechanoresponsive, is upregulated specifically in cancerous ducts. In contrast, filamin A, which is much less mechanoresponsive, is upregulated across the entire pancreatic tissue, including the stroma. These patterns were also noted in non-invasive lesions, termed pancreatic intraepithelial neoplasia (PanINs) (Fig. S2B), with increasing expression associated with cancer progression. Our results are largely in keeping with normal versus pancreatic cancer tissue datasets in the Gene Expression Omnibus (GEO) (Fig. S2C). The staining patterns are also consistent with the Human Protein Atlas, which tracks RNA and immunohistochemistry and which suggests that filamin B and α-actinin 4 are poor prognostic indicators for pancreatic cancer patients (49). Filamin A shows variable PDAC expression across these studies, and α-actinin 1 displays high staining in both normal and cancerous cells. Overall, the immunohistochemistry data indicate that, as a unit, the mechanoresponsive machinery is upregulated in the pancreatic ductal adenocarcinomas of patient tumors.

PDAC cell lines as a mechanoresponsive model for PDAC

To determine if PDAC cell lines can be used to study the changing mechanobiome landscape, we first assessed if the expression patterns that we observed in patient samples (Fig. 2) matched generally with changes between WT-like HPDE and various primary tumor and metastatically-derived lines. Western analysis across four lines revealed a general increase in myosin IIA and IIC, the disappearance of myosin IIB, and an increase in α-actinin 4 and filamin B, with moderate or unchanged levels of α-actinin 1 and filamin A (Fig. 3A–C, Table S1). To begin to develop a quantitative framework for the role of myosin IIs in pancreatic cancer, we measured the concentration of each myosin paralog in these pancreatic cancer-derived cells. We first calibrated both HeLa cells, which express myosin IIA and IIB, and AsPC-1 cells, which express myosin IIC, to generate a quantitative comparator for measuring each paralog's concentration across cell lines. To calibrate HeLa and AsPC-1 cells, we added purified paralog-specific myosin II tail fragments to the extract (Fig. S3A). From these calibration measurements, we calculated that the nonmuscle myosin IIA concentration in human pancreatic cells ranged from 540 nM in HPDE cells to 770 nM in Panc4.03 cells. These values compare favorably with the amounts of myosin II in budding yeast (Myo2p, 450 nM; Myp2p, 380 nM, (50)) and in *Dictyostelium discoideum* (Myo II, 3.4 μM, (51)) (Table S1). By comparison to myosin IIA, myosin IIB and IIC are found at much lower concentrations. Interestingly, myosin IIC increased 1.5-fold from approximately two percent of all myosin II in HPDE cells to about three percent of all myosin II in AsPC-1 cells, while myosin IIB decreased from ~8% of all myosin II in HPDEs to undetectable in AsPC-1 cells (Fig. 3A, Table S1). The dramatic change in myosin IIC in normal and cancerous ducts in the immunohistochemistry is consistent with the myosin quantification across PDAC cell lines (Fig. 2). Myosin IIC also exists in two splice variants and find that both variants increase in expression in AsPC-1 cells (Fig. S3B). While myosin IIC appears to be a minor myosin II paralog based on its concentration, in fact we find below that this paralog plays a major role in pancreatic cancer cell mechanics and behavior.

Modulation of cell mechanics through mechanoresponsive machinery and 4-HAP

We previously demonstrated that WT-like HPDE cells are less deformable than patient-derived PDAC cell lines (42). To determine if mechanoresponsive elements of the PDAC

mechanobiome contribute to this mechanical differential, we used micropipette aspiration (MPA) to measure the effective cortical tension (T_{eff}) of cells with overexpression or knockdown of myosin II, α-actinin, and filamin paralogs in Panc10.05 cells (Fig. 4A, Fig. S3A, C, D, E). Across all cell lines, knockdowns were 70–95% (Fig. S3C, E). Driving myosin IIA levels up or down yielded an altered cortical tension, which rose and fell with myosin IIA expression levels. Myosin IIB overexpression had no impact on cortical tension. Myosin IIB knockdowns were not pursued since Panc10.05 cells (as well as other PDAC lines and patient tissue samples) have no detectable levels of this protein (Fig. 3A, Fig. 2A, Fig. S2). Alpha-actinin 1 overexpression had no effect on cell mechanics, while both overexpression and knockdown of α-actinin 4 decreased the T_{eff} by half (Fig. 4A; Fig. S3C, D, E). Filamin A and B overexpressing cells ruptured under the applied pressures needed to measure cortical tension where the condition of $L_p=R_p$ must be met. However, filamin B knockdown cells could be measured and had an increase in cortical tension (Fig. 4A).

Interestingly, despite contributing only 3% of the overall myosin II in these cells (Table S1), overexpression and knockdown of myosin IIC had a profound impact on cell mechanics, leading to an overall reduction in cortical tension of 20% and 40%, respectively (Fig. 4A). Myosin IIC has a similar impact on mechanics in colorectal cancer cells, where it also constitutes a small percentage of the total myosin II (Bryan *et al.*, submitted for publication). To further explore the impact that myosin IIC has on the PDAC mechanobiome and cell mechanics, we used the small molecule 4-hydroxyacetophenone (4-HAP) which we previously identified in a *Dictyostelium* screen for mechanical modulators. In *Dictyostelium*, 4-HAP increased cortical tension by driving myosin II to the cell cortex. 4-HAP shows myosin II-paralog specificity in mammalian cells by increasing the assembly of myosin IIC (and IIB) and decreasing the deformability of several PDAC cell lines (42). Indeed, 4-HAP treatment increased the cortical tension of control cells where myosin IIC is present, but had no impact on myosin IIC-depleted cells (Fig. 4A). In addition, 4-HAP also extinguished the mechanoresponsiveness of myosin IIC in a dose-dependent manner, with no effect on myosin IIA mechanoresponsiveness (Fig. 1B). We also confirmed that 4-HAP treatment did not alter expression of the myosin II paralogs over a 24-hour window (Fig. S3F).

Knowing that the myosin II paralogs' mechanoresponsiveness was independent of each other (Fig. 1C, D), we tested how they might influence 4-HAP's ability to inhibit myosin IIC's mechanoresponse. The overexpression of myosin IIB or IIC did not affect myosin IIA's mechanoresponsiveness, even in the presence of 4-HAP (Fig. 1C). However, myosin IIB and myosin IIC's mechanoresponsiveness was still inhibited by 4-HAP even though myosin IIA was co-expressed with them (Fig. 1C, D). Furthermore, loss of myosin IIA does not alter myosin IIC's ability to assemble in cells, as assessed by sedimentation (Fig. S3G).

Our previous studies indicated that 4-HAP works by promoting assembly of myosin IIC and IIB (42). To further flesh out the concept that 4-HAP inhibits mechanoresponsiveness by driving over-assembly of myosin IIC, we asked whether driving assembly of myosin IIC in a different manner would also inhibit its mechanoresponsiveness. To do this, we expressed the human version of the myosin IIC tail fragment that corresponds to the mouse version, known to promote bipolar filament assembly (52). Indeed, expression of the myosin IIC tail fragment inhibited myosin IIC's mechanoresponsiveness phenocopying 4-HAP's effect (Fig.

1D). These observations further confirm that 4-HAP influences myosin IIC, and myosin IIB, independently of myosin IIA and does so by promoting bipolar filament assembly.

In concert with micropipette aspiration, which measures mechanical properties on the >500-ms time-scale (cortical tension measurements are performed over 10s of seconds), we used Real Time Deformability Cytometry (RT-DC) (53), which measures mechanics on the 4-ms timescale and across the whole cell (Fig. S4A). Reduction of myosin IIA, but not myosin IIC, increased cell deformation (Fig. 4B). The deformation was converted to an elastic modulus and calculated to be 1.17±0.37 kPa (mean±SD) for control, 1.07±0.3 kPa for shIIA, and 1.21±0.34 kPa for shIIC. This trending reduction (9%) in the elastic modulus measured for knockdown of myosin IIA, which is the most abundant paralog in the PDAC cells, is similar to the reduction in elasticity measured for WT versus *myoII* genetic deletion cells in *Dictyostelium* (54). The elastic modulus measured on short time-scales contrasts with the ~2-fold difference in cortical tension measured over longer time-scales, highlighting the complexity of the mechanical roles of these proteins (55). In addition, RT-DC reveals mechanical differences across pancreatic cancer cell lines (Fig. S4B).

Myosin IIC alters actin bundling and flow, facilitating dissemination

In addition to mediating mechanoresponsiveness (Fig. 1) and cell mechanics (Fig. 4), nonmuscle myosin II proteins also impact cytoskeletal arrangements and contractility. To determine how myosin IIC specifically impacts the cytoskeletal organization in collectives of cells, we generated tissue spheroids with knockdown Panc10.05 cell lines and examined the impact of 4-HAP treatment on those spheroids. Control knockdowns plated in 3D collagen I matrices showed partial dissemination, which was greatly increased in NMIIA knockdowns, similar to observations in other cancer models (56–58). In contrast, knockdown of myosin IIC showed no dissemination (Fig. 5A, **top row**). Upon treatment with 4-HAP for 24 hours, dissemination in both the control and NMIIA knockdown decreased, while no change was observed in the myosin IIC-depleted spheroids. To further analyze the fine-detail in cytoskeletal structures, spheroids were plated on collagen I-coated 2D substrates, and similar morphological differences were observed as in the 3D cultures (Fig. 5A, **middle row**). In addition, we observed tight actin cortical banding patterns on the periphery of the tumor spheroids in the absence of myosin IIC. This banding pattern was also observed in the control and NMIIA knockdown spheroids with 4-HAP treatment. To assess the actin redistribution, we used computer-assisted image analysis on the 2D spheroids and measured the continuity of banding, the percent coverage of actin filaments at the spheroid edge, and the homogeneity of the actin in those structures (calculated as the standard deviation of pixel intensity normalized to control) (Fig. S5). Across all analyses, myosin IIA knockdown spheroids had the least amount of discrete and continuous banding (Fig. 5B, Fig. S5A, B) and the least amount of actin staining at the tissue edge (Fig. S5C). Upon 4-HAP treatment, all of these metrics changed – more discrete and continuous belts emerged and the median percentage staining of actin increased 2-fold. By comparison, the myosin IIC knockdown tissue spheroids had discrete and continuous actin belts that remained unchanged upon 4-HAP addition (Fig. 5B, Fig. S5B, C), consistent with 4-HAP working primarily through myosin IIC. Interestingly, by these analytics, treatment with 4-HAP in the control tissue spheroids seemed to decrease discrete band formation.

We then used Structural Illumination Microscopy (SIM) to acquire higher resolution views of the structures along the tissue spheroid edges (Fig. 5A bottom row, Fig. 5B). In the control spheroids, the actin belts are formed by the structural rearrangement of the actin bundles. Specifically, 4-HAP induces a coarser distribution of actin composed of dense actin belts and leads to the emergence of filopodial-like structures or retraction fibers. In the myosin IIA knockdowns treated with 4-HAP, tight actin belts, as well as elaborate arrays of parallel actin bundles, are also clearly visible. In contrast, myosin IIC knockdowns had elaborate peripheral actin structures that were largely unchanged between untreated and 4-HAP-treated samples. Thus, 4-HAP induces alterations in peripheral actin structures in a myosin IIC-dependent manner.

To address myosin IIC's role in actin rearrangements, we next determined its cellular localization. In tissue spheroids, fluorescently-labeled myosin IIC is both diffusely localized throughout the cell and along actin filaments (Fig. 5C). When actin filaments collapse to form actin belts upon 4-HAP treatment, myosin IIC shows strong co-localization with those belts. In single Panc10.05 and AsPC-1 cells, endogenous myosin IIC is predominately confined to the cell cortex including in actin-rich protrusions, whereas myosin IIA localizes along stress fibers (Fig. 5C). In single cells, 4-HAP decreases the number of actin-rich protrusions, as measured with our edge detection algorithm (Fig. 5D, E, Fig. S6). Similarly, in tissue spheroids, 4-HAP induced peripheral actin belts that are rich in myosin IIC (Fig. 5F).

Overall, this analysis highlights two major findings. First, in collections of cells, despite being present in small quantities, myosin IIC plays a major role in mediating actin network structural rearrangements and dynamics. Myosin IIA, known to contribute to retrograde actin flow, may work in concert with myosin IIC to drive these cytoskeletal rearrangements. Second, 4-HAP reduces the fluidity of the network: by stabilizing actin belt structures in a manner independent of myosin IIA, but dependent on myosin IIC. Thus, by altering the actin cytoskeleton, 4-HAP inhibits dissemination from tissue spheroids.

Because retrograde flow moves actin filaments away from the cell perimeter, we hypothesized that the cortical actin belts could be formed by a reduction in this flow. Therefore, we examined the impact of 4-HAP on retrograde actin flow by staining live cells with SiR-actin and observing the actin network using lattice light sheet microscopy (Fig. S6A) and confocal microscopy. Most 4-HAP-treated cells had undetectable levels of actin flow, as observed by Kymograph (Fig. 5G, Fig. S6B). Those cells in which retrograde flow could be measured showed a 50% reduction in velocity over untreated controls (Fig. 5H, Movies S1, S2). In addition, cells treated with 4-HAP showed an increase in bleb formation (Fig 5H, **inset**). This large and measurable impact on actin dynamics explains in part the dose-dependent decrease on trans-well migration in control and myosin IIA knockdown AsPC-1 cells (Fig. 5I). Overall, 4-HAP's reduction of actin flow, cell dissemination, and invasion indicates its potential for preventing PDAC metastasis.

4-HAP decreases PDAC metastatic potential in mice

Critical regulators of myosin II have significantly altered expression associated with pancreatic cancer progression and in pancreatic cancer-derived cell lines (19,39,41). These

genetic alterations suggest that myosin II, particularly myosin IIC whose expression is specifically elevated in malignant pancreatic ductal epithelia, may be an attractive target for modulating PDAC cell behavior. Therefore, we tested 4-HAP in a mouse model of PDAC using hemisplenectomy, which simulates the metastatic process in the liver. In this model, the spleen is separated into halves and tumor cells are injected into one half, which is then removed after the tumor cells have entered the liver to prevent local injection-site tumor formation. Mice develop micrometastases in 1–2 weeks and gross disease by 3–4 weeks. Athymic *NCr-nu/nu* mice with AsPC-1 liver metastases were divided into three groups: control (untreated), PBS (200 μl PBS IP injections, every other day), and 4-HAP (5 mg/ml, 200 μl IP injections, every other day). Mice were sacrificed at 5-weeks post-surgery, when the first mouse expired. Metastases to the liver were observed and quantified using our custom Matlab script, which measures surface area tumor coverage (Fig. 6A). Results from both liver weights and tumor coverage show that 4-HAP treatment led to a 50% reduction in tumor formation (Fig. 6B, Fig. S7).

Discussion

A cell's ability to react to changing mechanical and chemical cues in its environment depends on the adaptability of its mechanobiome. Increased contractility and altered deformability, as well as rapid turnover of cytoskeletal proteins, are trademarks of cells responding to constantly changing surroundings. Gene expression programs are upregulated to provide cells with added adaptability at specific time points in developing embryos, and differentiating cells show increased expression of mechanoresponsive proteins during mechanically turbulent periods. For example, filamin's mechanoresponsiveness is required for maturation of actin-rich ring canals that interconnect the nurse cells and oocyte in developing *Drosophila* egg chambers (59), and filamin B is upregulated in embryonic vascular endothelial cells (60). Both α-actinin 1 and α-actinin 4 show temporally defined expression in developing zebrafish embryos, with both expressed in the notochord and α-actinin 4 also expressed in the developing gut (61). Each of the nonmuscle myosin II paralogs have roles in development as well, including but not limited to neurite outgrowth and maturation (NMIIB and NMIIC) (62), nephron development (NMIIA and NMIIB) (*e.g.* (63)), and hearing (NMIIA) (64).

In the mechanobiome, forces are shared between myosin II and different actin crosslinkers, with myosin II having potentiating or inhibitory effects on certain crosslinkers and vice versa (12,54). This mechanosensory system constitutes a control system, where mechanical inputs can be converted to signaling outputs in a manner analogous to chemical signal transduction (45). Through our work (12), an important delineation has emerged: the cell has at least two systems of proteins that when depleted, lead to alterations in cortical viscoelasticity and tension. One set of proteins leads to increased mechanoresponsiveness, while the other set of proteins leads to reduced mechanoresponsiveness. Cells that mature into terminally differentiated tissues often readjust the cytoskeletal milieu to favor reduced mechanoresponsiveness over their developmental program. These stable expression patterns, however, are altered in precancerous cells (often caused by upstream genetic lesions), and revert cells to programs activated in early development that endow them again with

increased adaptability. In fact, supporting cells of the tumor, the pancreatic stellate cells, also become highly adaptable, a trait which can be targeted to reduce tumor cell invasion (8).

The mechanobiome of the cancerous ductal cells plays an essential role in cell shape change, leading to PDAC invasion and metastasis (Fig. 7A). Specifically, the mechanoresponsive proteins myosin IIA, myosin IIC, α-actinin 4, and filamin B are upregulated in patient-derived tissues (Fig. 7B), where they alter the structural arrangement of the actin cytoskeleton and impact cell mechanics to facilitate metastasis (Fig. 7C). In addition, despite its low abundance, myosin IIC plays an important role in facilitating actin organization and retrograde flow. Also, our data on myosin IIC suggest that changes in the expression level of minor proteins that are often discounted in larger data mining may in fact, be worthy of reconsideration, given the large impact myosin IIC has on cell mechanics and cell behavior. Our *in vivo* metastasis assays demonstrate that the myosin IIA-IIC dynamic can be fine-tuned towards a therapeutic benefit with mechanical modulators such as 4-HAP (Fig. 7D). In addition, because myosin IIC is specifically upregulated in ductal adenocarcinoma cells, the pharmacological modulation of this protein is unlikely to negatively impact healthy pancreatic tissue; 4-HAP should synergize with other strategies such as immunological intervention in pancreatic cancer patients, since immune cells do not typically express myosin IIC (42). In fact, enhanced activation of T cells on stiffer substrates suggests that 4-HAP, which stiffens the immunological target cells, could behave as an excellent immunotherapy adjuvant (65).

In summary, the observations presented here imply that targeting cancer by broadening strategies to include small molecule mechanical modulators can have significant effects by reducing metastatic potential. Modulation of mechanoresponsive proteins has several advantages. First, we can fine-tune the activity of proteins that are upregulated in cancerous tissue, thus harnessing the cell's intrinsic protein make-up to revert them to more normal phenotypes, while protecting healthy cells that do not upregulate these targeted proteins. Second, this strategy draws upon the normal biochemistry of the protein to overwhelm the mechanics of the system. In our studies, we are hitting on both concepts: We are using 4-HAP to increase the assembly of myosin IIC, which is specifically upregulated in PDAC, in order to overcome the protein's innate adaptive ability. 4-HAP treatment pushes myosin IIC to lock onto the cytoskeletal network, thus inhibiting the tumor cell's ability to polarize and reorganize its actin cytoskeleton. This concept is reinforced by the actin structural remodeling observed in colorectal cancer cells presented in our companion paper by Bryan *et al.* (submitted for publication). Overall, incorporating the mechanobiome as a targetable drug space in combination with other therapeutic approaches is a valuable strategy for reducing PDAC metastases (Fig. 7).

Supplementary Material

Refer to Web version on PubMed Central for supplementary material.

Acknowledgments

References

1. Remmerbach TW, Wottawah F, Dietrich J, Lincoln B, Wittekind C, Guck J. Oral cancer diagnosis by mechanical phenotyping. Cancer Res 2009;69:1728–32 [PubMed: 19223529]

2. Cross SE, Jin YS, Rao J, Gimzewski JK. Nanomechanical analysis of cells from cancer patients. Nat Nanotechnol 2007;2:780–3 [PubMed: 18654431]

3. Staunton JR, Doss BL, Lindsay S, Ros R. Correlating confocal microscopy and atomic force indentation reveals metastatic cancer cells stiffen during invasion into collagen I matrices. Sci Rep 2016;6:19686 [PubMed: 26813872]

4. Biomechanics Suresh S. and biophysics of cancer cells. Acta Biomater 2007;3:413–38 [PubMed: 17540628]

5. Kim TH, Gill NK, Nyberg KD, Nguyen AV, Hohlbauch SV, Geisse NA, et al. Cancer cells become less deformable and more invasive with activation of beta-adrenergic signaling. J Cell Sci 2016;129:4563–75 [PubMed: 27875276]

6. Nguyen AV, Nyberg KD, Scott MB, Welsh AM, Nguyen AH, Wu N, et al. Stiffness of pancreatic cancer cells is associated with increased invasive potential. Integr Biol (Camb) 2016;8:1232–45 [PubMed: 27761545]

7. Kai F, Drain AP, Weaver VM. The Extracellular Matrix Modulates the Metastatic Journey. Dev Cell 2019;49:332–46 [PubMed: 31063753]

8. Chronopoulos A, Robinson B, Sarper M, Cortes E, Auernheimer V, Lachowski D, et al. ATRA mechanically reprograms pancreatic stellate cells to suppress matrix remodelling and inhibit cancer cell invasion. Nat Commun 2016;7:12630 [PubMed: 27600527]

9. Laklai H, Miroshnikova YA, Pickup MW, Collisson EA, Kim GE, Barrett AS, et al. Genotype tunes pancreatic ductal adenocarcinoma tissue tension to induce matricellular fibrosis and tumor progression. Nat Med 2016;22:497–505 [PubMed: 27089513]

10. Chronopoulos A, Lieberthal TJ, Hernandez AED. Pancreatic cancer: a mechanobiology approach. Converg Sci Phys Onc 2017;3

11. Discher DE, Janmey P, Wang YL. Tissue cells feel and respond to the stiffness of their substrate. Science 2005;310:1139–43 [PubMed: 16293750]

12. Luo T, Mohan K, Iglesias PA, Robinson DN. Molecular mechanisms of cellular mechanosensing. Nat Mater 2013;12:1064–71 [PubMed: 24141449]

13. Schiffhauer ES, Luo T, Mohan K, Srivastava V, Qian X, Griffis ER, et al. Mechanoaccumulative Elements of the Mammalian Actin Cytoskeleton. Curr Biol 2016;26:1473–9 [PubMed: 27185555]

14. Torrino S, Roustan FR, Kaminski L, Bertero T, Pisano S, Ambrosetti D, et al. UBTD1 is a mechano-regulator controlling cancer aggressiveness. EMBO Rep 2019;20

15. Broders-Bondon F, Nguyen Ho-Bouldoires TH, Fernandez-Sanchez ME, Farge E. Mechanotransduction in tumor progression: The dark side of the force. J Cell Biol 2018;217:1571–87 [PubMed: 29467174]

16. Salvi AM, DeMali KA. Mechanisms linking mechanotransduction and cell metabolism. Curr Opin Cell Biol 2018;54:114–20 [PubMed: 29902730]

17. Kassianidou E, Kalita J, Lim RYH. The role of nucleocytoplasmic transport in mechanotransduction. Exp Cell Res 2019;377:86–93 [PubMed: 30768931]

18. Schiffhauer E, Robinson DN. Mechanochemical signaling directs cell-shape change. Biophys J 2017;112:207–14 [PubMed: 28122209]

19. Jones S, Zhang X, Parsons DW, Lin JC, Leary RJ, Angenendt P, et al. Core signaling pathways in human pancreatic cancers revealed by global genomic analyses. Science 2008;321:1801–6 [PubMed: 18772397]

20. Maimaiti Y, Tan J, Liu Z, Guo Y, Yan Y, Nie X, et al. Overexpression of cofilin correlates with poor survival in breast cancer: A tissue microarray analysis. Oncol Lett 2017;14:2288–94 [PubMed: 28781665]

21. Pappa KI, Lygirou V, Kontostathi G, Zoidakis J, Makridakis M, Vougas K, et al. Proteomic Analysis of Normal and Cancer Cervical Cell Lines Reveals Deregulation of Cytoskeleton-associated Proteins. Cancer Genomics Proteomics 2017;14:253–66 [PubMed: 28647699]

22. Wang WS, Zhong HJ, Xiao DW, Huang X, Liao LD, Xie ZF, et al. The expression of CFL1 and N-WASP in esophageal squamous cell carcinoma and its correlation with clinicopathological features. Dis Esophagus 2010;23:512–21 [PubMed: 20095995]

23. Kikuchi S, Honda K, Tsuda H, Hiraoka N, Imoto I, Kosuge T, et al. Expression and gene amplification of actinin-4 in invasive ductal carcinoma of the pancreas. Clin Cancer Res 2008;14:5348–56 [PubMed: 18765526]

24. Fukumoto M, Kurisu S, Yamada T, Takenawa T. alpha-Actinin-4 enhances colorectal cancer cell invasion by suppressing focal adhesion maturation. PLoS One 2015;10:e0120616 [PubMed: 25860875]

25. Honda K, Yamada T, Hayashida Y, Idogawa M, Sato S, Hasegawa F, et al. Actinin-4 increases cell motility and promotes lymph node metastasis of colorectal cancer. Gastroenterology 2005;128:51–62 [PubMed: 15633123]

26. Liu X, Chu KM. alpha-Actinin-4 promotes metastasis in gastric cancer. Lab Invest 2017;97:1084–94 [PubMed: 28581489]

27. Shiraishi H, Fujiwara Y, Kakuya T, Tsuta K, Motoi N, Miura N, et al. Actinin-4 protein overexpression as a predictive biomarker in adjuvant chemotherapy for resected lung adenocarcinoma. Biomark Med 2017

28. Gao Y, Li G, Sun L, He Y, Li X, Sun Z, et al. ACTN4 and the pathways associated with cell motility and adhesion contribute to the process of lung cancer metastasis to the brain. BMC Cancer 2015;15:277 [PubMed: 25885339]

29. Yamaguchi H, Ito Y, Miura N, Nagamura Y, Nakabo A, Fukami K, et al. Actinin-1 and actinin-4 play essential but distinct roles in invadopodia formation by carcinoma cells. Eur J Cell Biol 2017

30. Iguchi Y, Ishihara S, Uchida Y, Tajima K, Mizutani T, Kawabata K, et al. Filamin B Enhances the Invasiveness of Cancer Cells into 3D Collagen Matrices. Cell Struct Funct 2015;40:61–7 [PubMed: 25925610]

31. Steinhardt AA, Gayyed MF, Klein AP, Dong J, Maitra A, Pan D, et al. Expression of Yes-associated protein in common solid tumors. Hum Pathol 2008;39:1582–9 [PubMed: 18703216]

32. Bai H, Zhu Q, Surcel A, Luo T, Ren Y, Guan B, et al. Yes-Associated Protein impacts adherens junction assembly through regulating actin cytoskeleton organization. Am J Physiol - Gastrointest Liver Phys 2016;311:G369–G411

33. Maitra A, Adsay NV, Argani P, Iacobuzio-Donahue C, De Marzo A, Cameron JL, et al. Multicomponent analysis of the pancreatic adenocarcinoma progression model using a pancreatic intraepithelial neoplasia tissue microarray. Mod Pathol 2003;16:902–12 [PubMed: 13679454]

34. Sun Q, Luo T, Ren Y, Florey O, Shirasawa S, Sasazuki T, et al. Competition between human cells by entosis. Cell Res 2014;24:1299–310 [PubMed: 25342560]

35. Yang X, Cao W, Zhou J, Zhang W, Zhang X, Lin W, et al. 14-3-3zeta positive expression is associated with a poor prognosis in patients with glioblastoma. Neurosurgery 2011;68:932–8 [PubMed: 21242845]

36. Tang Y, Lv P, Sun Z, Han L, Luo B, Zhou W. 14-3-3zeta up-regulates hypoxia-inducible factor-1alpha in hepatocellular carcinoma via activation of PI3K/Akt/NF-small ka, CyrillicB signal transduction pathway. Int J Clin Exp Pathol 2015;8:15845–53 [PubMed: 26884855]

37. Su CH, Zhao R, Zhang F, Qu C, Chen B, Feng YH, et al. 14-3-3sigma exerts tumor-suppressor activity mediated by regulation of COP1 stability. Cancer Res 2011;71:884–94 [PubMed: 21135113]

38. Tong S, Xia T, Fan K, Jiang K, Zhai W, Li JS, et al. 14-3-3zeta promotes lung cancer cell invasion by increasing the Snail protein expression through atypical protein kinase C (aPKC)/NF-kappaB signaling. Exp Cell Res 2016;348:1–9 [PubMed: 27554601]

39. Zhou Q, Kee Y-S, Poirier CC, Jelinek C, Osborne J, Divi S, et al. 14-3-3 coordinates microtubules, Rac and myosin II to control cell mechanics and cytokinesis. Curr Biol 2010;20:1881–9 [PubMed: 20951045]

40. West-Foyle H, Kothari P, Osborne J, Robinson DN. 14-3-3 proteins tune non-muscle myosin II assembly. J Biol Chem 2018;293:6751–61 [PubMed: 29549125]

41. Jhaveri DT, Kim MS, Thompson ED, Huang L, Sharma R, Klein AP, et al. Using Quantitative Seroproteomics to Identify Antibody Biomarkers in Pancreatic Cancer. Cancer Immunol Res 2016;4:225–33 [PubMed: 26842750]

42. Surcel A, Ng WP, West-Foyle H, Zhu Q, Ren Y, Avery L, et al. Pharmacological activation of myosin II paralogs to correct cell mechanics defects. Proc Natl Acad Sci U S A 2015;112:1428–33 [PubMed: 25605895]

43. Deng Y, Davis SP, Yang F, Paulsen KS, Kumar M, Sinnott DeVaux R, et al. Inertial Microfluidic Cell Stretcher (iMCS): Fully Automated, High-Throughput, and Near Real-Time Cell Mechanotyping. Small 2017;13

44. Effler JC, Kee YS, Berk JM, Tran MN, Iglesias PA, Robinson DN. Mitosis-specific mechanosensing and contractile-protein redistribution control cell shape. Curr Biol 2006;16:1962–7 [PubMed: 17027494]

45. Kee YS, Ren Y, Dorfman D, Iijima M, Firtel RA, Iglesias PA, et al. A mechanosensory system governs myosin II accumulation in dividing cells. Mol Biol Cell 2012;23:1510–23 [PubMed: 22379107]

46. Luo T, Mohan K, Srivastava V, Ren Y, Iglesias Pablo A, Robinson Douglas N. Understanding the cooperative interaction between myosin II and actin cross-linkers mediated by actin filaments during mechanosensation. Biophys J 2012;102:238–47 [PubMed: 22339860]

47. Schiffhauer ES, Ren Y, Iglesias VA, Kothari P, Iglesias P, Robinson DN. Myosin IIB assembly state determines its mechanosensitive dynamics. J Cell Biol 2019;218:895–908 [PubMed: 30655296]

48. Beach JR, Shao L, Remmert K, Li D, Betzig E, Hammer JA, 3rd. Nonmuscle myosin II isoforms coassemble in living cells. Curr Biol 2014;24:1160–6 [PubMed: 24814144]

49. Uhlen M, Zhang C, Lee S, Sjostedt E, Fagerberg L, Bidkhori G, et al. A pathology atlas of the human cancer transcriptome. Science 2017;357

50. Wu J-Q, Pollard TD. Counting cytokinesis proteins globally and locally in fission yeast. Science 2005;310:310–4 [PubMed: 16224022]

51. Robinson DN, Cavet G, Warrick HM, Spudich JA. Quantitation of the distribution and flux of myosin-II during cytokinesis. BMC Cell Biol 2002;3:4 [PubMed: 11860600]

52. Ronen D, Rosenberg MM, Shalev DE, Rosenberg M, Rotem S, Friedler A, et al. The positively charged region of the myosin IIC non-helical tailpiece promotes filament assembly. J Biol Chem 2010;285:7079–86 [PubMed: 19959848]

53. Otto O, Rosendahl P, Mietke A, Golfier S, Herold C, Klaue D, et al. Real-time deformability cytometry: on-the-fly cell mechanical phenotyping. Nat Methods 2015;12:199–202 [PubMed: 25643151]

54. Reichl EM, Ren Y, Morphew MK, Delannoy M, Effler JC, Girard KD, et al. Interactions between myosin and actin crosslinkers control cytokinesis contractility dynamics and mechanics. Curr Biol 2008;18:471–80 [PubMed: 18372178]

55. Robinson DN, Kee Y-S, Luo T, Surcel A. Understanding how dividing cells change shape In: Egelman EH, editor. Comprehensive Biophysics. Oxford: Academic Press; 2012 p 48–72.

56. Liu T, Ye Y, Zhang X, Zhu A, Yang Z, Fu Y, et al. Downregulation of nonmuscle myosin IIA expression inhibits migration and invasion of gastric cancer cells via the cJun Nterminal kinase signaling pathway. Mol Med Rep 2016;13:1639–44 [PubMed: 26719067]

57. Schramek D, Sendoel A, Segal JP, Beronja S, Heller E, Oristian D, et al. Direct in vivo RNAi screen unveils myosin IIa as a tumor suppressor of squamous cell carcinomas. Science 2014;343:309–13 [PubMed: 24436421]

58. Conti MA, Saleh AD, Brinster LR, Cheng H, Chen Z, Cornelius S, et al. Conditional deletion of nonmuscle myosin II-A in mouse tongue epithelium results in squamous cell carcinoma. Sci Rep 2015;5:14068 [PubMed: 26369831]

59. Huelsmann S, Rintanen N, Sethi R, Brown NH, Ylanne J. Evidence for the mechanosensor function of filamin in tissue development. Sci Rep 2016;6:32798 [PubMed: 27597179]

60. Zhou X, Tian F, Sandzen J, Cao R, Flaberg E, Szekely L, et al. Filamin B deficiency in mice results in skeletal malformations and impaired microvascular development. Proc Natl Acad Sci U S A 2007;104:3919–24 [PubMed: 17360453]

61. Holterhoff CK, Saunders RH, Brito EE, Wagner DS. Sequence and expression of the zebrafish alpha-actinin gene family reveals conservation and diversification among vertebrates. Dev Dyn 2009;238:2936–47 [PubMed: 19842183]

62. Wylie SR, Chantler PD. Myosin IIC: a third molecular motor driving neuronal dynamics. Mol Biol Cell 2008;19:3956–68 [PubMed: 18614800]

63. Recuenco MC, Ohmori T, Tanigawa S, Taguchi A, Fujimura S, Conti MA, et al. Nonmuscle Myosin II Regulates the Morphogenesis of Metanephric Mesenchyme-Derived Immature Nephrons. J Am Soc Nephrol 2015;26:1081–91 [PubMed: 25168025]

64. Lalwani AK, Atkin G, Li Y, Lee JY, Hillman DE, Mhatre AN. Localization in stereocilia, plasma membrane, and mitochondria suggests diverse roles for NMHC-IIa within cochlear hair cells. Brain Res 2008;1197:13–22 [PubMed: 18241845]

65. Hui KL, Balagopalan L, Samelson LE, Upadhyaya A. Cytoskeletal forces during signaling activation in Jurkat T-cells. Mol Biol Cell 2015;26:685–95 [PubMed: 25518938]

Author Manuscript

Author Manuscript

Author Manuscript

Author Manuscript

Statement of Significance:
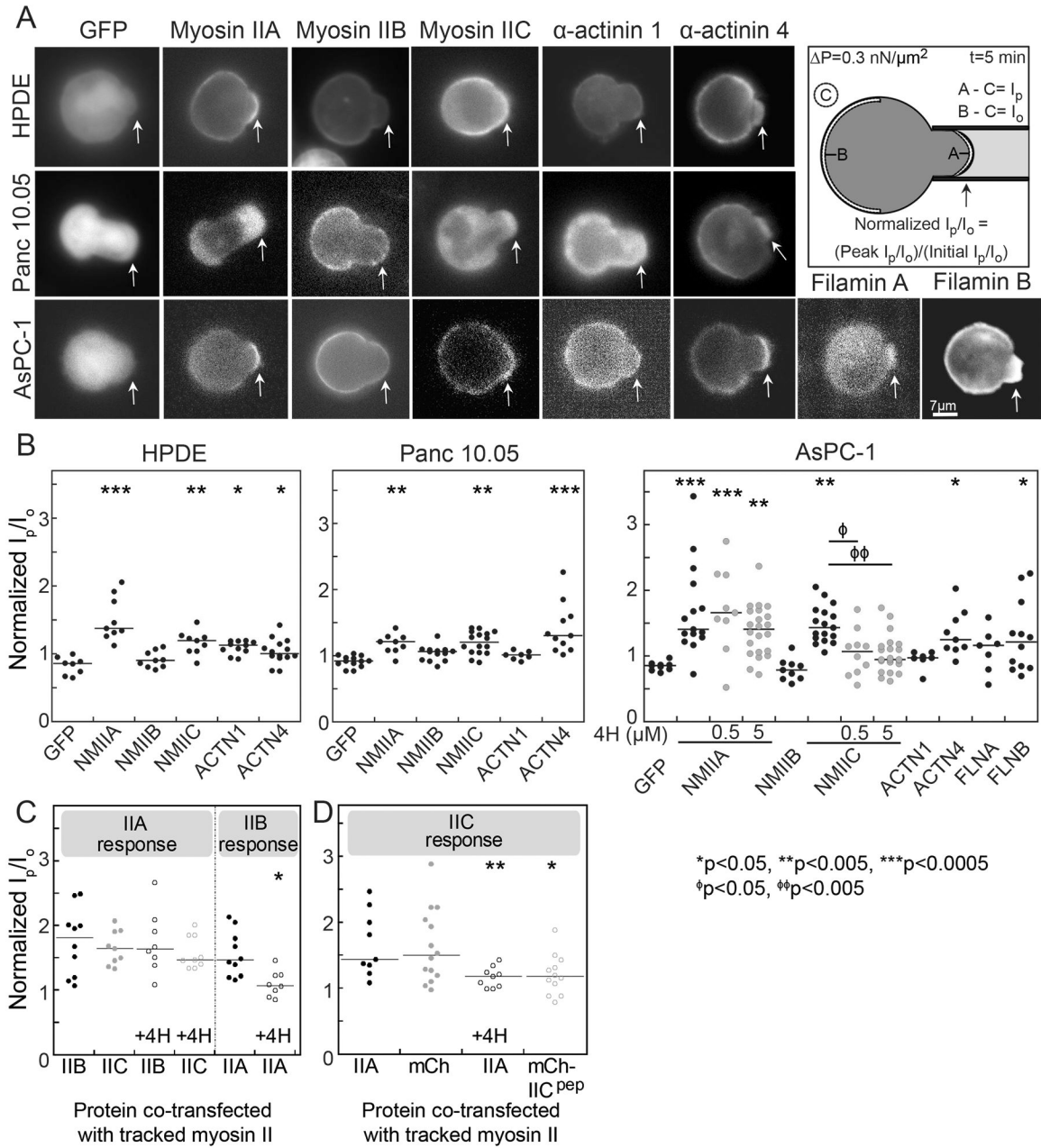
Mechanoresponsive proteins are upregulated during pancreatic cancer progression and can be pharmacologically targeted to inhibit metastasis.

Fig. 1: Nonmuscle myosin IIA, myosin IIC, α-actinin 4, and filamin B show mechanoresponsiveness in pancreatic cancer cells.

A. Representative images across HPDE, Panc10.05, and AsPC-1 cell lines of the maximum accumulation of GFP alone, GFP-labeled myosin IIs, α-actinin 4, filamin A, and filamin B, and mCherry-α-actinin 1, show peak intensity after applied stress in MPA mechanoresponse experiments. Arrows identify regions where mechanical stress was applied. Scale bar, 7 μm. Cartoon shows how mechanoresponse is calculated. **B**. Quantification of mechanoresponsiveness normalized as a ratio of fluorescence intensity at the tip (I_p) to the intensity at the opposite cortex (I_o), both in the absence of and the presence of two different concentrations of 4-HAP. **C, D**. Quantification of mechanoresponsiveness of myosin IIA and

IIB normalized as an I_p/I_o ratio in HeLa cells co-transfected with different myosin paralogs in the presence and absence of 500 nM 4-HAP. We used HeLa cells here because myosin IIB is mechanoresponsive in these cells (13,47). **D**. In addition, quantification of myosin IIC co-transfected with a small myosin IIC peptide known to induce IIC assembly is provided. Medians plotted; *p<0.05, **p<0.005, ***p<0.0005.
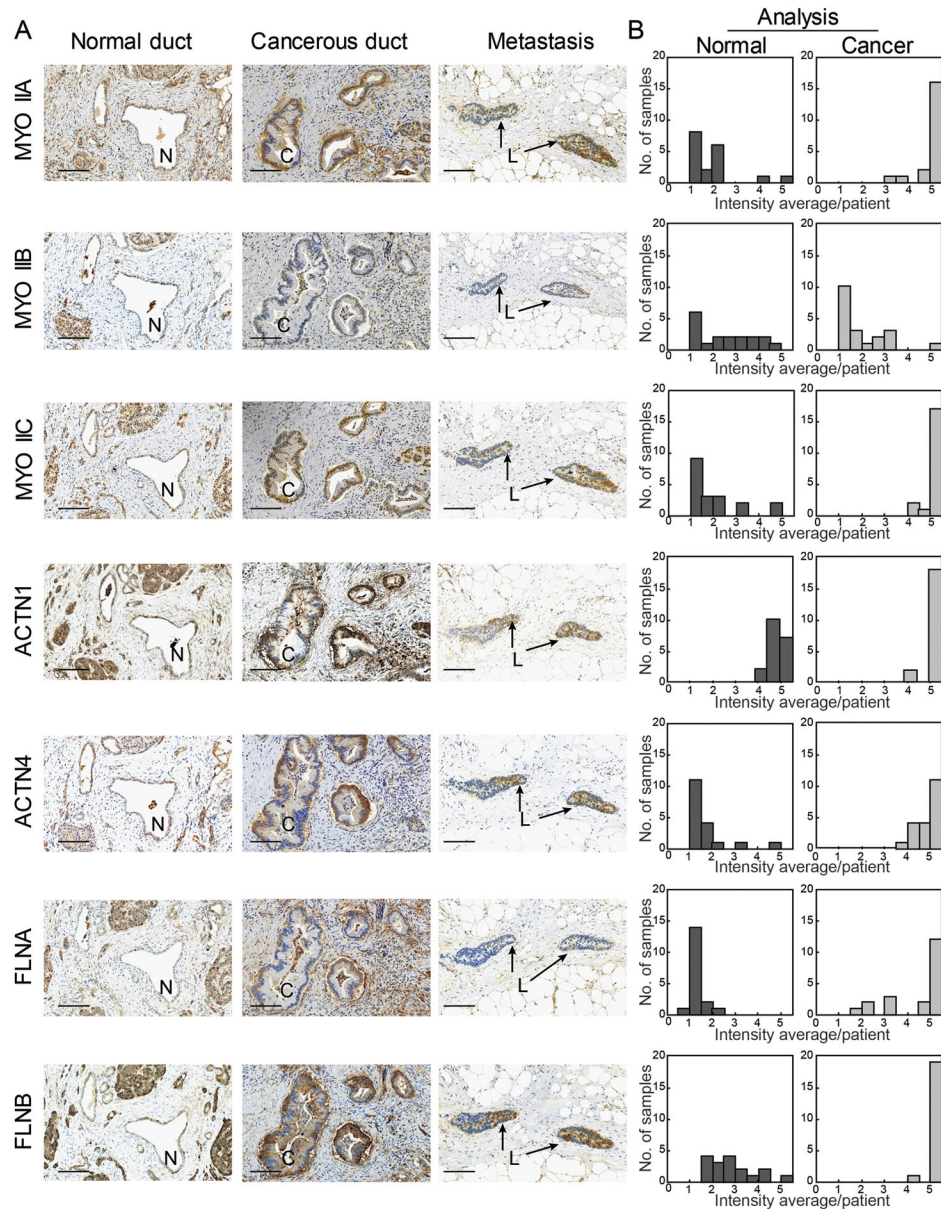
Fig. 2: The mechanoresponsive machinery is elevated in pancreatic ductal adenocarcinoma in human pancreatic tissue.

A. Immunohistochemistry staining of pancreatic tissue from human PDAC patients shows increased expression in the cancerous ducts of mechanoresponsive proteins nonmuscle myosin IIA and IIC, α-actinin 4, and both filamin A and B. Scale bar = 100 μm. For each sample – normal duct (**N**), cancerous duct (**C**), and metastatic lesion (**L**) – the same site is shown across all seven antibodies stained. In addition, both the normal and cancerous ducts are from the same patient. **B**. Quantification of staining intensity and surface area across 20 patients illustrate an up-regulation of mechanoresponsive proteins, as well as filamin A. Data are plotted as a histogram of the intensity average per patient (described in Fig. S1A and Materials and Methods) across the study group.
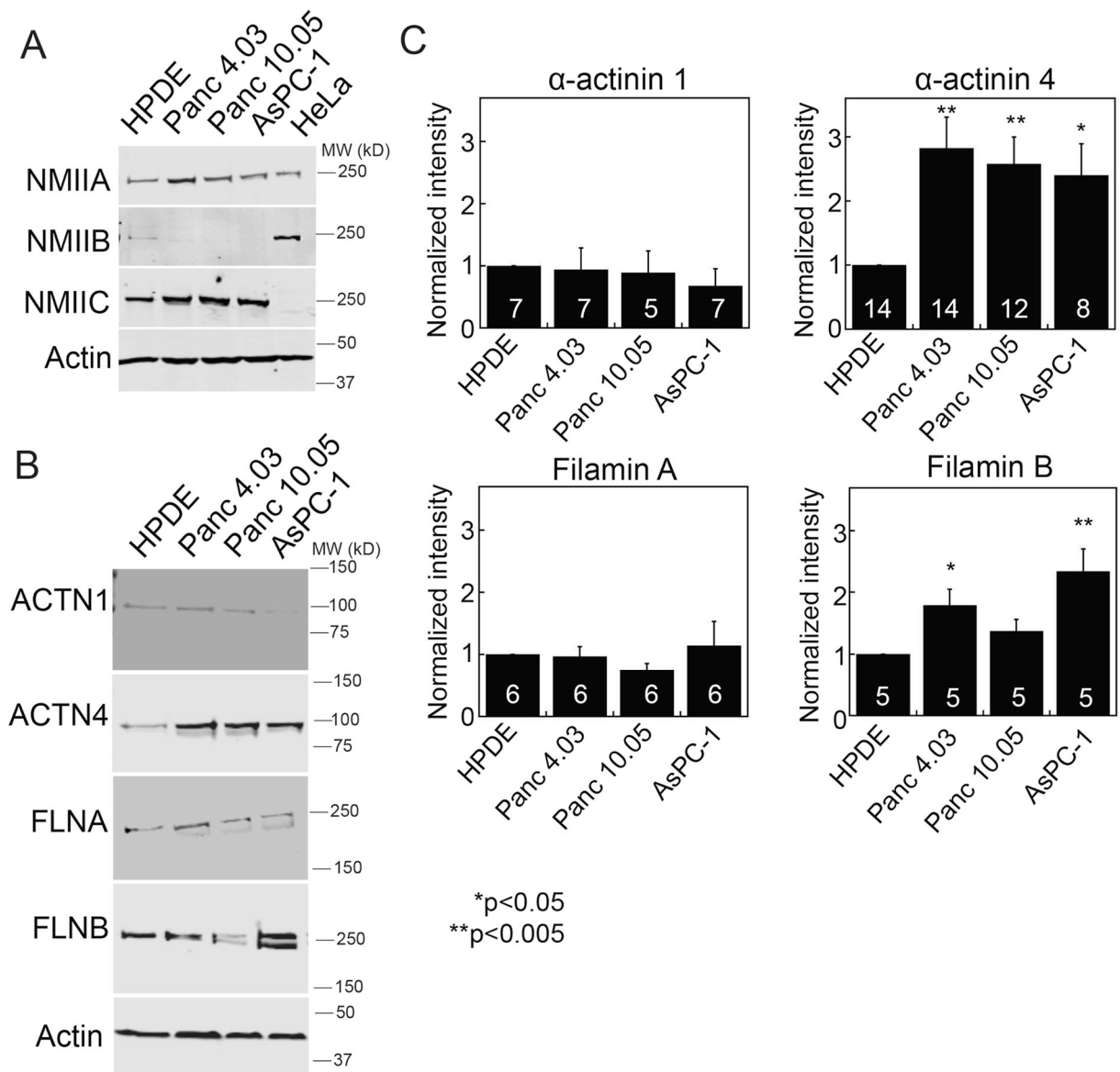
Fig. 3: Mechanoresponsive proteins increase in pancreatic cancer-derived cell lines.
A. Expression of myosin IIA (NMIIA), myosin IIB (NMIIB), myosin IIC (NMIIC), and actin in HPDE (normal pancreatic ductal epithelium), Panc4.03 (stage II primary tumor), Panc10.05 (stage II primary tumor), and AsPC-1 (stage IV ascites metastasis) cells, compared with HeLa lysate for the purposes of quantification. NMIIA and NMIIC increase in expression, while NMIIB decreases in expression in cancer cell lines. For full quantification of myosin II paralogs, see Table S1. **B**. Expression of α-actinin 4 (ACTN4) and filamin B (FLNB) increase, while expression of α-actinin 1 (ACTN1) and filamin A (FLNA) do not change in cancer cell lines. **C**. Quantification of western blots, examples shown in **B**, where numbers on the bars indicate n-values. *p<0.05, **p<0.005.
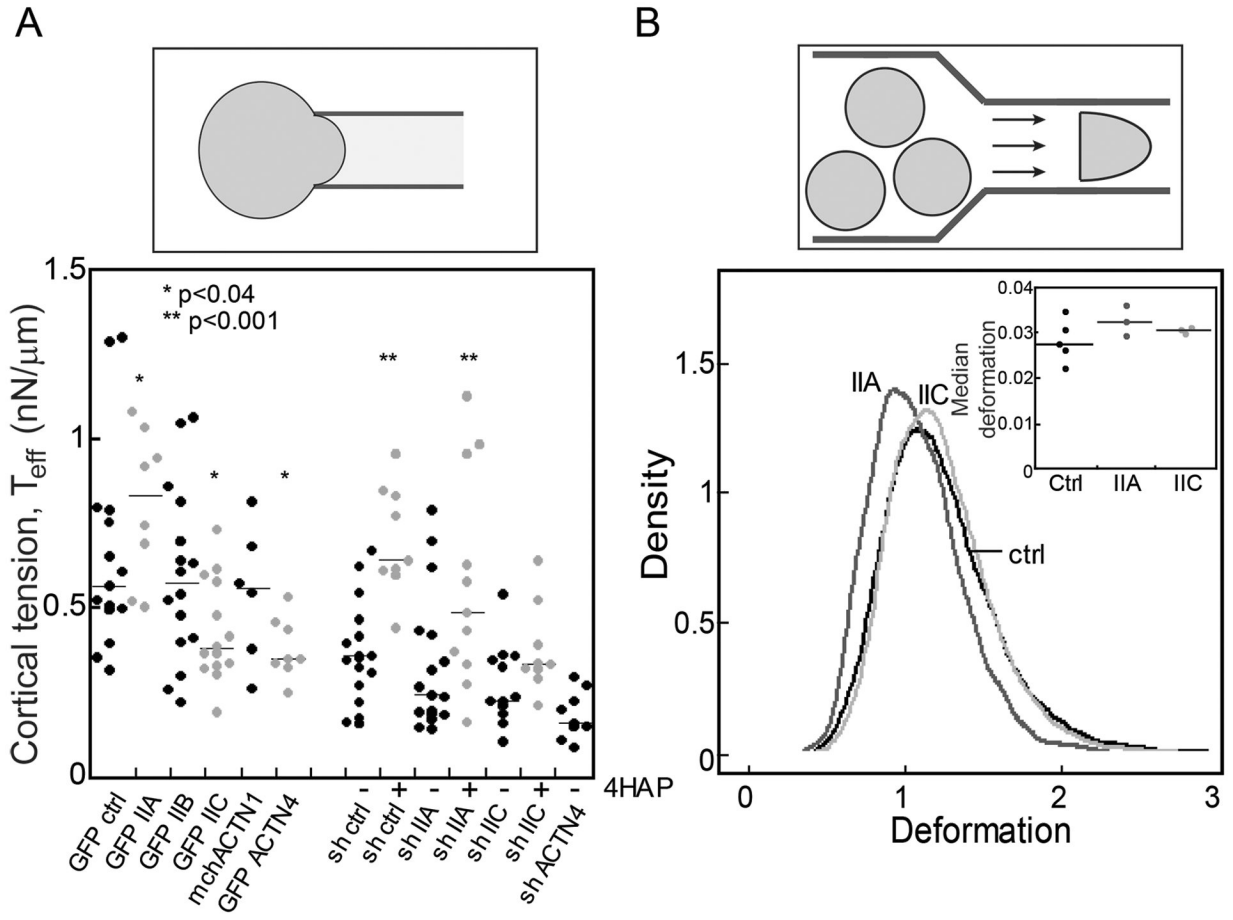
Fig. 4: Mechanoresponsive proteins impact cortical tension and deformability of PDAC cells.
A. The effective cortical tension (T_{eff}) measured by MPA experiments (schematic) is significantly affected by overexpression of myosin IIA, myosin IIC, and α-actinin 4, all mechanoresponsive paralogs. 500 nM 4-HAP increases the cortical tension of sh-control cells. 4-HAP also increases the cortical tension in myosin IIA knockdown cells, whose primary myosin paralog myosin IIC is activated by 4-HAP (42). Knockdown of myosin IIC also leads to a decrease in cortical tension, unchanged by 4-HAP challenge. Medians plotted; * p<0.03; **p<0.0001 relative to control. **B**. RT-DC experiments (schematic) demonstrate increased deformation when myosin IIA and myosin IIC are knocked-down (plotted as a probability distribution). All cell lines are generated from Panc10.05 cells. N=7521 cells for control, 9632 cells for myosin IIA knockdown, and 5933 cells for myosin IIC knockdown. Cell types are distinct (p<0.0001). Inset: Median deformation of three to five RT-DC independent runs across cell types from which the elastic modulus was calculated. Average median deformation values are 0.027±0.002 (mean±SD) for ctrl, 0.032±0.002 for IIA knockdown, and 0.031±0.0003 for IIC knockdown.
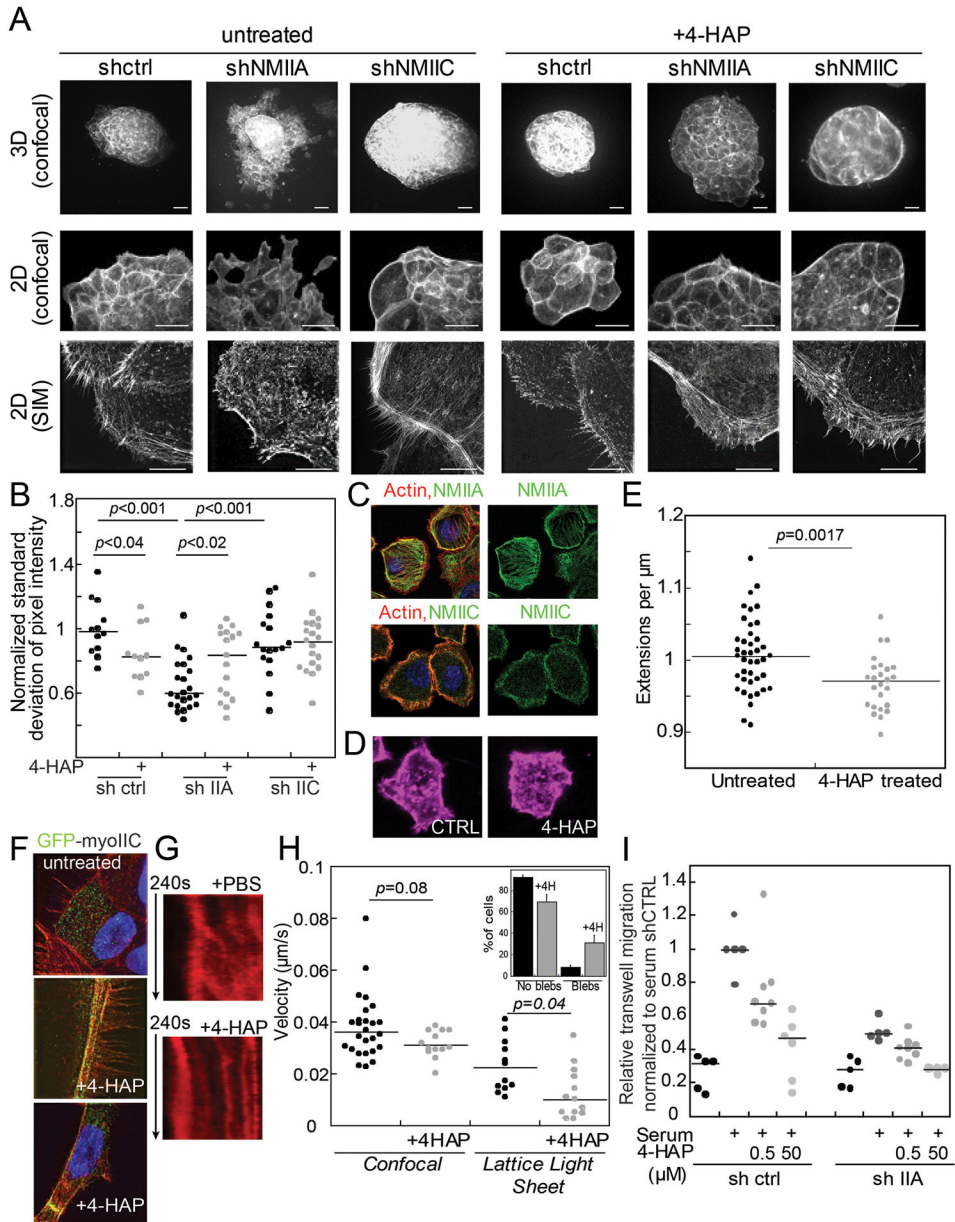
Fig. 5: Myosin IIC alters cytoskeletal actin architecture and cell behavior upon 4-HAP treatment.

A. Panc10.05 tissue spheroids grown, stained with phalloidin, and imaged in 3D (Matrigel) or 2D (collagen) show dissemination, exacerbated in myosin IIA knockdown. Myosin IIC depletion suppresses dissemination and generates actin cortical belts. 4-HAP induces actin belts in control and myosin IIA-depleted spheroids. These belts are already present in myosin IIC-depleted spheroids. Scale bar, 40 μm (confocal); 10 μm (SIM). **B**. Quantification of these actin structures using normalized standard deviation of pixel intensity; see **Methods**. Medians plotted; p values on graphs. **C**. Endogenous myosin IIA in AsPC-1 cells localizes on actin stress fibers; myosin IIC localizes to the actin cortex. **D**. 4-HAP reduces the number of extensions formed by AsPC-1 cells. **E**. Numbers of extensions/μm of

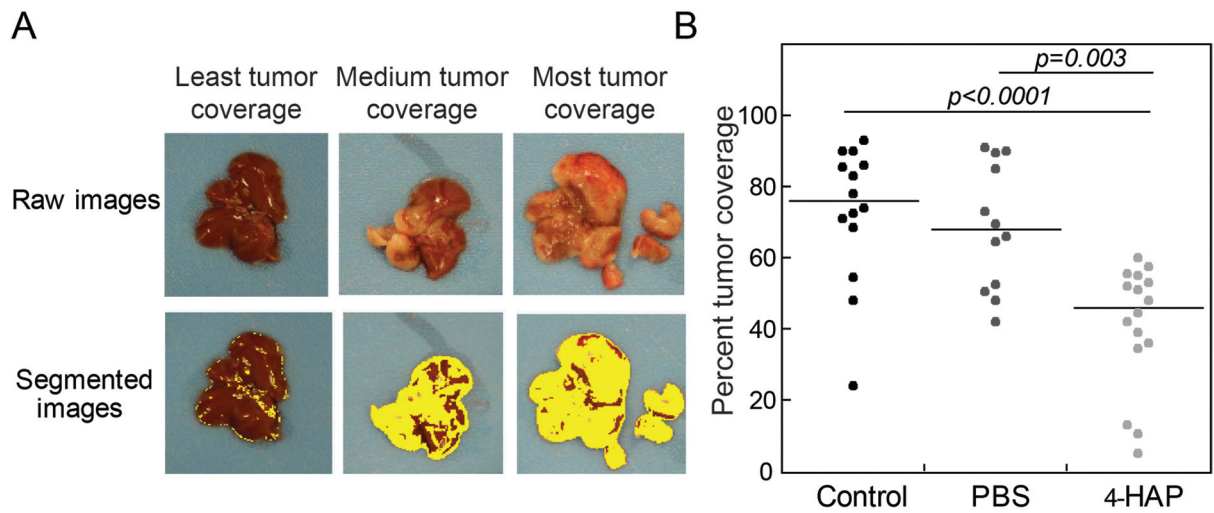perimetric distance are plotted. **F**. GFP-myosin IIC decorates actin filaments, especially actin belts induced by 4-HAP in tissue spheroids. **G**. Sample kymographs of line scans across active leading edges in AsPC-1 SirAct live-stained cells. **H**. 4-HAP decreases retrograde flow. Medians are plotted. Inset shows increase in bleb formation in 4-HAP-treated cells (p=0.0028). **I**. AsPC-1 shCTRL and shIIA cells show dose-dependent reduction of transwell migration upon 4-HAP treatment. Medians are shown.

A

Least tumor   Medium tumor   Most tumor
coverage   coverage   coverage

Raw images

Segmented
images

B

Fig. 6: 4-HAP reduces PDAC liver metastasis in murine model.
Livers harvested from 4-HAP-treated mice that underwent hemi-splenectomies with AsPC-1 cells show a reduction in tumor coverage over those livers from untreated mice. **A**. Images were quantified using image segmentation based on color gradients to discern tumor coverage (Fig. S5). **B**. Quantification of tumor coverage show a 50% reduction in surface tumor load. Medians are provided on the graph.
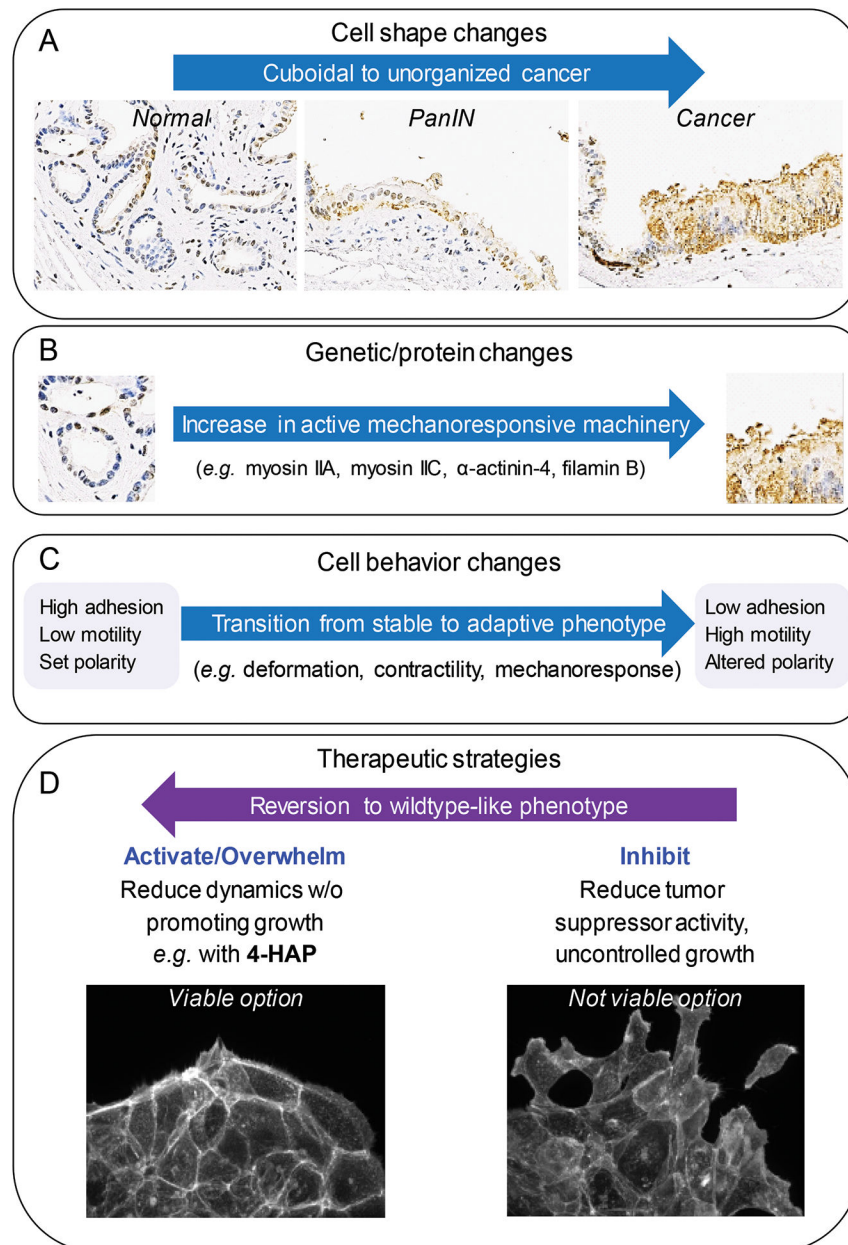
Fig. 7: New therapeutic strategy: Ablate metastasis by overwhelming intrinsic machinery to prevent polarization.

A. Pancreatic cancer progression is histologically defined by a series of cell shape change events from cuboidal epithelial cells (normal), through pseudo-stratified epithelial layers (PanIn), to disorganized and prolific cell growth (cancer). **B**. These changes are concomitant with genetic lesions and alterations in protein expression, including those proteins that define the mechanoresponsive machinery in PDAC, primarily myosin IIA, myosin IIC, α-actinin-4, and filamin B. These changes in mechanoresponsive machinery have (**C**) significant implications on cell behavior moving the system from a stable state with high cellular adhesion, low motility, and set polarity, to an adaptive state with low adhesion, high motility, and altered polarity. **D**. Common therapeutic approaches have primarily involved

inhibiting key proteins. This loss of activity is not a viable approach for the PDAC mechanobiome because it leads to uncontrolled growth and dissemination as seen in myosin IIA inhibition or knockdown. Instead, we propose activating or overwhelming the system with mechanical modulators such as 4-HAP which revert the system to a more wildtype-like phenotype, reducing the dynamics of the system without promoting uncontrolled growth.